

1 **Diverging hydrological drought traits over Europe with global warming**

2

3 Carmelo Cammalleri*, Gustavo Naumann, Lorenzo Mentaschi, Bernard Bisselink, Emiliano Gelati,
4 Ad De Roo and Luc Feyen

5

6 European Commission, Joint Research Centre (JRC), 21027 Ispra (VA), Italy.

7 * Correspondence: carmelo.cammalleri@ec.europa.eu; Tel.: +39-0332-78-9869.

8

9 **Abstract**

10 Climate change is anticipated to alter the demand and supply of water at the earth's surface. Since
11 many societal impacts from a lack of water happen under drought conditions, it is important to
12 understand how droughts may develop with climate change. This study shows how hydrological
13 droughts will change across Europe with increasing global warming levels (GWL of 1.5, 2 and 3 K
14 above preindustrial temperature). We employed a low-flow analysis based on river discharge
15 simulations of the LISFLOOD spatially-distributed physically-based hydrological and water use
16 model, which was forced with a large ensemble of regional climate model projections under a high
17 emissions (RCP8.5) and moderate mitigation (RCP4.5) pathway. Different traits of drought,
18 including severity, duration and frequency, were investigated using the threshold level method. The
19 projected changes in these traits identify four main sub-regions in Europe that are characterized by
20 somehow homogeneous and distinct behaviours with a clear southwest/northeast contrast. The
21 Mediterranean and Boreal sub-regions of Europe show strong, but opposite, changes at all three
22 GWLs, with the former area mostly characterized by stronger droughts (with larger differences at 3
23 K) while the latter is expected to experience a reduction in all drought traits. In the Atlantic and
24 Continental sub-regions the changes are expected to be less marked and characterized by a larger
25 uncertainty, especially at the 1.5 and 2 K GWLs. Combining the projections in drought hazard with
26 population and agricultural information shows that with 3 K global warming an additional 11

27 million people and 4.5 million ha of agricultural land are projected to be exposed to droughts every
28 year, on average, with the most affected areas located in the Mediterranean and Atlantic regions of
29 Europe.

30

31 **Keywords:** climate change, LISFLOOD, drought, low-flow analysis, Paris agreement, global
32 warming levels, human water use

33 **1. Introduction**

34 As a natural phenomenon, drought occurs in all climates due to a temporary lack of
35 precipitation, which can propagate through the different compartments of the water cycle (Van
36 Loon and Van Lanen, 2012). Drought conditions can be exacerbated by high temperatures, causing
37 an increase in evapotranspiration demand and soil water content draining (e.g., Teuling et al., 2013),
38 and their impacts can be further intensified in areas with an overexploitation of available water
39 resources (Van Loon and Van Lanen, 2013). The strong dependency of drought conditions on the
40 key meteorological forcing suggests likely effects of climate change on future drought severity,
41 duration and frequency, mainly through an alteration of the water balance dynamics (Stagl et al.,
42 2014).

43 Depending on the degree of penetration of the water deficit into the hydrological cycle,
44 drought is commonly classified into meteorological (e.g., precipitation), agricultural (e.g., soil
45 moisture) and hydrological (e.g., river discharge) drought (Wilhite, 2000). Each drought type may
46 be perceived most relevant for a specific application, and different indicators may capture different
47 effects of climate change (Feng, 2017). In spite of the strong connection between the socioeconomic
48 impacts of droughts and negative soil moisture and river discharge anomalies, fewer studies (e.g.,
49 Samaniego et al., 2018; Forzieri et al., 2014) have focused on the impact of climate change on
50 agricultural and hydrological droughts at European scale compared to meteorological events (e.g.,
51 Heinrich and Gobiet, 2012; Spinoni et al., 2018). This focus on meteorological drought mainly
52 relates to the relative simplicity and lower input data requirements of calculating meteorological
53 drought indicators (i.e., Standardised Precipitation Index, SPI) compared to agricultural and
54 hydrological drought indices, whose analysis usually requires simulations from hydrological
55 models, as also highlighted by the larger emphasis placed on meteorological drought hazard in
56 operational monitoring systems (Barker et al., 2016). Scientific and practical interest in
57 hydrological drought is motivated by the direct and indirect impacts on several socioeconomic
58 sectors, such as energy production, inland water transportation (Meyer et al., 2013), irrigated

59 agriculture, and public water supply (see the European Drought Impact Inventory,
60 <https://www.geo.uio.no/edc/droughtdb/>), as well as causing losses of ecosystem and biodiversity
61 (Crausbay and Ramirez, 2017). In particular, streamflow drought complements meteorological and
62 soil moisture droughts thanks to its more rapid response to precipitation aberrations compared to
63 groundwater (Tallaksen and van Lanen, 2004).

64 With the raising awareness of climate change, a number of local and regional studies assessed
65 the potential impacts of climate change on hydrological drought in recent years (e.g., Brunner et al.,
66 2019; Cervi et al., 2018; Hellwig and Stahl, 2018; Nerantzaki et al., 2019; Rudd et al., 2019; Van
67 Tiel et al., 2018). These studies provided highly detailed insights on the local processes, but the
68 limited extent of their spatial domain and lack of homogeneity in the adopted drought indicators,
69 modelling framework and climate scenarios complicated the understanding of large-scale patterns
70 of changes. In spite of the value of continental-scale analyses, few studies have looked at how
71 hydrological droughts could develop across Europe with climate change. They are typically based
72 on pan-European hydrological models forced by climate projections (Feyen and Dankers, 2009;
73 Forzieri et al., 2014; Lehner et al., 2006; Marx et al., 2018; Roudier et al., 2016), with ever
74 improved representation of processes in the hydrological models. These improvements included
75 accounting for the effects of water use, more detail in the climate projections (by the use of higher
76 resolution regional climate models), and better accounting for climate uncertainty through multi-
77 model ensembles.

78 Most past studies portrayed how drought conditions across Europe could look at future points
79 in time (mid- or end- of century) for alternative scenarios of greenhouse gas emissions. However,
80 following the UNFCCC (United Nations Framework Convention on Climate Change) Paris
81 Agreement (UNFCCC, 2015) and the focus on limiting the increase in global average temperature
82 to well below 2 K above the pre-industrial level, the paradigm in climate change studies has started
83 to shift from analysing the effects at specific future time windows to evaluating the effect at specific
84 global warming levels (GWLs). To date, there are only few studies that provided insights on how

85 hydrological droughts could change at different GWLs. Roudier et al. (2016) used three
86 hydrological models forced with high resolution regional climate projections to evaluate changes in
87 10- and 100-year streamflow drought events, with a focus solely on the 2 K scenario. Marx et al.
88 (2018) used three different hydrological models forced by coarse-resolution global climate
89 projections that were downscaled accounting for altitude effects in temperature and precipitation.
90 They used a simple 90-th percentile of exceedance of river discharge as index, which is
91 representative of the low-flow spectrum. Both studies did not consider water consumption, which is
92 key to represent feedbacks between droughts and human activities (Van Loon et al., 2016).

93 To further deepen the understanding of the influence of climate change and water use on
94 future droughts, the daily streamflow simulations for the pan-European river network obtained with
95 the LISFLOOD spatially-distributed hydrological model, forced with an ensemble of 11 bias-
96 corrected regional climate projections for RCP4.5 and RCP8.5 (Moss et al., 2010), were used. The
97 model incorporates water use modules to reproduce the major sectorial water demands, accounting
98 for the human impact on streamflow propagation, and resulting in a streamflow deficit that
99 represents the integrated deficiency in water availability over the entire upstream catchment.

100 These streamflow simulations were analysed with the twofold goal of: i) evaluate changes in
101 hydrological droughts across Europe between present climate and climate corresponding to
102 different GWLs, and ii) quantify the effects of the projected changes on two of the main exposed
103 compartments. Specifically, we look at 1.5, 2 and 3 K global warming, which represent the different
104 Paris agreement climate change mitigation targets, and we exploited the threshold level method for
105 event extraction, which allows for a detailed extreme value analysis of different streamflow drought
106 traits, including severity, duration and frequency. The effects of the projected changes on two key
107 exposed quantities is also evaluated through a drought exposure analysis, with a specific focus on
108 the changes between the present and future exposed population and agricultural land, which are
109 representative quantities in the major social and economic sectors impacted by drought in Europe
110 (e.g., agriculture and livestock farming, and public water supply).

111 **2. Materials and Methods**

112 **2.1 Climate forcing**

113 In this study, we used projections from 11 combinations of global and regional climate models
114 under two Representative Concentration Pathways (RCP4.5 and RCP8.5) obtained from the EURO-
115 CORDEX initiative (Jacob et al., 2014). The climate projections used in this study were produced
116 by Dosio (2020) by applying a bias-correction quantile mapping approach (Dosio et al., 2012) using
117 the observational dataset EOBSv10 (Haylock et al., 2008). The analysis focused on 30-year time
118 windows centred on the year when the global models project an increase in global average
119 temperature of 1.5, 2 and 3 K above preindustrial (1881-1910) temperature. For these periods,
120 drought characteristics were contrasted against those derived for the baseline reference period
121 (1981-2010), which has a 0.7 K temperature increase compared to the preindustrial period.

122 Across all models, the two RCPs reach the 1.5 and 2 K GWLs around the year 2030 and 2053
123 (RCP4.5), 2025 and 2040 (RCP8.5), on average. The RCP8.5 simulations reach the 3 K GWL in
124 2063 on average, whereas only one model reaches 3 K warming for RCP4.5. According to the
125 independence of the projected river flow changes from the adopted pathway observed in Mentaschi
126 et al. (2020) for annual minimum (drought), average and maximum (flood) flows, we assumed that
127 a single multi-model ensemble can be obtained by merging the outputs from both RCPs. Given that
128 only one model reaches 3 K warming for RCP4.5, the model ensemble was composed by a total of
129 22 members for the 1.5 and 2 K GWLs and only 12 members for the 3 K GWL.

130 **2.2 Hydrological modelling**

131 Simulations of daily river discharge (Q) were produced at a 5×5 km spatial resolution over
132 Europe by forcing the LISFLOOD model (De Roo, 2000) with the bias-corrected climate
133 projections. LISFLOOD is a spatially-distributed physically-based hydrological model that
134 simulates all the main hydrological processes occurring in the land-atmosphere system, including
135 evapotranspiration fluxes (separately for crop transpiration and direct evaporation), infiltration

136 (Xinjiang model), soil water redistribution in the vadose zone (Darcy 1-D vertical flow model),
137 groundwater dynamics (two parallel linear reservoirs), snow accumulation and melt (degree-day
138 factor method) and surface runoff (for further details on each module, see Burek et al., 2013). The
139 surface runoff generated in each cell is channelled to the nearest river network cell by means of a
140 routing component based on a 4-point implicit finite-difference solution of the kinematic wave
141 (Chow et al., 1988).

142 The water abstractions component in LISFLOOD consist of five modules: (manufacturing)
143 industrial, energy, livestock, domestic and irrigation water demand. While irrigation water demand
144 is modelled dynamically within LISFLOOD, the other four components are downscaled to the
145 model grid cells from country-level data obtained from EUROSTAT and AQUASTAT. High
146 resolution data from the Land-Use based Integrated Sustainability Assessment (LUISA) Territorial
147 Modelling Platform (Jacobs-Crisioni et al., 2017) were used for the spatial downscaling.

148 In detail, irrigation was estimated dynamically at the model time step (daily in this study)
149 based on two distinct methods for crop irrigation and paddy-rice irrigation, as defined from land use
150 maps. In the former, the demanded water amount by the crop (transpiration) is compared to the
151 available water in the soil and the irrigation is modelled to keep the soil water content at field
152 capacity (also accounting for the different efficiency of the irrigation systems). In the paddy-rice
153 irrigation instead, a defined water-level is maintained during the whole irrigation season (also
154 accounting for soil percolation).

155 Livestock water demand at grid scale was modelled as described in Mubareka et al. (2013), by
156 computing the water demand of each livestock category (e.g., cattle, pigs, sheep) from livestock
157 density maps and literature water requirements. Public water withdrawal was downscaled to model
158 resolution using a land use proxy approach (Vandecasteele et al., 2014), assuming that public water
159 withdrawal is the total water withdrawn in populated areas (i.e., water usage from
160 commercial/service are negligible). Similarly, industrial water demand was disaggregated using the
161 industry/commerce land use class in the LUISA platform (Bisselink et al., 2018), Water demand for

162 energy and cooling was computed with a relatively similar approach, with national data downscaled
163 to the locations of large power thermal power stations registered in the European Pollutant Release
164 and Transfer Register data base (E-PRTR).

165 Future projections of the main socioeconomic drivers of water use are based on the EU
166 economic, budgetary, and demographic projections (EC, 2015), and the European energy reference
167 scenario (Capros et al., 2013) available in the LUISA platform. Irrigation demand was modelled
168 based on projected agriculture land use changes and the dynamic climate-dependent water
169 requirements. Projections of future industrial water demand were based on the Gross Value Added
170 of the industrial sector available from the GEM-E3 model (Capros et al., 2013). Future changes in
171 energy water use were simulated according to the electricity consumption projections from the
172 POLES model (Prospective Outlook on Long-term Energy Systems, Keramidas et al., 2017). Future
173 domestic water demand was estimated based on spatially detailed (100 × 100 m) projected
174 population maps. Due to the absence of information on future livestock in LUISA, the
175 corresponding water demand was kept constant. Considering the relatively limited extent of area
176 with high livestock water demand (Mubareka et al., 2013), only small effects are expected due to
177 this assumption. As the EU projections do not go up to the end of the end of the century, projections
178 of water use are dynamic only up to 2050 and were kept constant afterwards.

179 The LISFLOOD modelling framework have been successfully applied in Feyen and Dankers
180 (2009) and Forzieri et al. (2014) in previous studies on drought future projections. In these analyses,
181 model simulations were validated against long records (more than 30 years) of streamflow data
182 from several gauging stations (209 and 446 stations, respectively), obtaining satisfactory results on
183 quantities such as annual minima and deficit. Gauging stations were mostly located in western and
184 central Europe, where both studies highlighted less reliable performances during the frost season.

185 The most recent calibration and validation exercise of LISFLOOD over the European domain
186 has been performed over more than 700 stations as part of the EFAS (<https://www.efas.eu/>) flood
187 early warning systems (Arnal et al., 2019). The calibration procedure is based on the Evolutionary

188 Algorithm described in Hirpa et al. (2018), and it adopted the Kling-Gupta Efficiency (KGE; Gupta
189 et al., 2009) as the objective function in order to target an optimization of three quantities: total
190 volume, the spread of the flow (e.g. flow duration curve), and the timing and shape of the
191 hydrograph (Yilmaz et al., 2008).

192 **2.3 Drought modelling**

193 The hydrological drought modelling approach used in this study is analogous to the
194 methodology used to estimate the low-flow indicator developed as part of the European Drought
195 Observatory (EDO) (Cammalleri et al., 2017). The key quantity is the water deficit computed from
196 an unbroken sequence of discharge (Q) values below a defined low-flow threshold. We used the 85-
197 th percentile of exceedance, Q_{85} , derived for the present climate as a threshold both in the present
198 and future scenarios, with the aim to estimate how droughts under present climate conditions will be
199 projected under climate change.

200 According to the theory of runs (Yevjevich, 1967), a continuous period with river flow values
201 below the defined low-flow threshold was considered as a drought event, of which the severity was
202 quantified by the total deficit (D , represented by the area enclosed between the threshold and the
203 streamflow time series). Other key traits of drought derived from the analysis were the duration,
204 quantified by the length of the drought in days (N), and the frequency of the events, which can be
205 expressed as return period (T).

206 In order to avoid potential bias in the analysis with the inclusion of minor events and to ensure
207 the independence among events, two post-processing corrections were applied after selection of the
208 events below the threshold: 1) small isolated events (of duration less than 5 days) were removed
209 from the analysis (Jakubowski and Radczuk, 2004), and 2) consecutive events with an inter-event
210 time smaller than 10 days were pooled together (Zelenhasić and Salvai, 1987).

211 Following this drought definition, a sequence of events for both the baseline period and the
212 three GWLs was derived. Given the large variability of D values across the European domain due to

213 differences in hydrological regimes and size of river basins, the changes in drought severity were
214 expressed as relative differences (%) from the values in the baseline period (1981-2010). The series
215 of D events was fitted according to the Pareto Type II distribution (also known as Lomax
216 distribution, a special case of the Generalized Pareto Distribution), formally expressed as (Lomax,
217 1987):

$$218 \quad F(D; \alpha, \lambda) = 1 - \left(1 + \frac{D}{\lambda}\right)^{-\alpha} \quad (1)$$

219 where α and λ are the strictly positive shape and scale parameters, respectively, derived from the
220 sample according to the maximum likelihood method. The fitted distributions allowed computing
221 the return period associated to a specific D value (T , the average occurrence interval which refers to
222 the expected value of the number of realizations to be awaited before observing an event whose
223 magnitude exceeds D ; Serinaldi, 2015), or to be used in reverse to estimate the D value associated
224 to a specific return period.

225 The same drought modelling approach was previously tested in Cammalleri et al. (2017) and
226 Cammalleri et al. (2020) for the development of a low-flow indicator as part of the European and
227 Global Drought Observatories (EDO and GDO, <https://edo.jrc.ec.europa.eu>). These tests included
228 assessments for some major past drought events, as well as goodness-of-fit test for the Lomax
229 distribution for both European and Global river basins. Within EDO and GDO, regular monthly
230 drought reports are also produced in case of significant drought events
231 (<https://edo.jrc.ec.europa.eu/edov2/php/index.php?id=1051>), which also systematically evaluate the
232 capability of the low-flow index to capture the dynamic of hydrological droughts.

233 **2.4 Population and agricultural land exposed to streamflow drought**

234 In order to quantify how global warming could change exposure to streamflow drought in
235 Europe, different exposed quantities can be analysed depending on the impacted sector. Among the
236 15 impact categories available in the European Drought Impact Inventory (EDII,

237 <https://www.geo.uio.no/edc/droughtdb/>), agriculture and livestock farming (category 1), and public
238 water supply (category 7) are the two most reported sectors. As a consequence, we decided to focus
239 the exposure analysis on population and agricultural land, as quantities strongly related to these two
240 categories. For the baseline we used the map of agricultural areas from the CORINE land Cover
241 (EEA, 2016) and the population density from the LUISA Territorial Modelling Platform (Batista e
242 Silva et al., 2013). Consistently with the water use simulations with socioeconomic dynamics up to
243 2050, for future exposure the LUISA land use and population projections of 2050 were used.

244 The spatial data of population and agricultural land were summed over NUTS 2 statistical
245 regions (or equivalent for EU-neighbour countries according to EUROSTAT,
246 <https://ec.europa.eu/eurostat/web/nuts/statistical-regions-outside-eu>). Similarly, the median change
247 in drought frequency of an event with a 10-year return period in the baseline was computed from all
248 the cells within a NUTS 2 region. These quantities allowed computing the expected changes in
249 exposed population and agricultural land, which were then equally divided over the 10-year period
250 to obtain a standardized year-average quantity. Finally, changes over NUTS 2 regions were further
251 aggregated to country scale.

252 **3. Results**

253 ***3.1 Evaluation of the changes in main drought traits***

254 ***3.1.1 Drought severity***

255 Figure 1 shows the ensemble-median relative change in severity of a 10-year drought between
256 the baseline and the GWLs, with positive (negative) values indicating a higher (lower) drought
257 severity with warming compared to the reference. In order to assess the robustness of the ensemble
258 median values, the projected changes are considered robust only if at least 2/3 of the ensemble
259 members agree on the sign of change (no-agreement otherwise), which is a simplification of the
260 approach proposed by Tebaldi et al. (2011) and applied over Europe by Dosio and Fischer (2018).

261 The spatial maps depicted in Figure 1 highlight a strong divergence in the projected changes of
262 drought severity with warming over Europe, with four macro-regions (delimited in Figure 1 lower-
263 right panel) displaying somewhat homogeneous behaviour. The four macro-regions were derived by
264 computing for each country the predominant change for the three GWLs, then by combining the
265 countries with similar features. These macro-regions are in line with the ones defined in the IPCC
266 AR5 subdivision for Europe (Kovats et al., 2014; Metzger et al., 2005), and they have been already
267 used in previous early studies at continental-scale (i.e., Feyen and Dankers, 2009; Lehner et al.,
268 2006). These four macro-regions are adopted in all the subsequent analyses.

269 In the Mediterranean sub-region (i.e., Iberian Peninsula, Italy, Greece and the Balkans)
270 generally more severe droughts are projected, whereas in the Boreal sub-area (i.e., Scandinavia
271 peninsula and Baltic countries) drought severity is expected to reduce almost everywhere. The
272 projected changes are less marked in two transition regions, but, in general, they point towards more
273 severe droughts in the Atlantic sub-region (i.e., British Isles, France, Belgium and the Netherlands)
274 and less severe droughts over the Continental sub-area (Germany, Poland and eastern European
275 countries). Overall, these patterns of change become stronger and more robust with increasing
276 warming.

277 The strongest increase in drought severity is projected for Portugal, Spain and Greece, where
278 the fraction of rivers with an increase in deficit of more than 50% at 3 K is 99, 80 and 75%,
279 respectively. If climate stabilizes at 2 K, streamflow drought severity is lower than at 3 K, but still
280 at least 50% higher than in the baseline for half of the rivers of Portugal and Spain, and 35% of
281 Greece. Capping global warming at 1.5 K would further limit the increase in severity, with only 21,
282 20 and 14% of the rivers of Portugal, Spain and Greece expected to experience an increase in
283 drought severity of more than 50%.

284 Over the Atlantic region (apart from Iceland), streamflow droughts are generally projected to
285 also become more severe with global warming. The south of France shows a pattern towards more

286 severe flow deficits with warming that is similar to that projected for most of the Mediterranean.
287 For the other parts of the Atlantic sub-region the changes are less pronounced. Keeping warming to
288 2 K or below would limit the increase in severity for most of the region to below 25% compared to
289 the baseline. At 3 K warming, the increase in severity could reach up to 50%. In some parts of the
290 Atlantic sub-region, such as the Seine river catchment in France (northern France), at lower levels
291 of warming the climate models do not agree on the sign of the change, or show a small trend
292 towards less severe droughts. Yet, with stronger warming the signal of change reverses towards
293 more severe droughts.

294 Over most of the Continental sub-region there is a trend towards less severe droughts with
295 global warming. On the one hand, this trend is somewhat more pronounced in upstream Danube
296 tributaries that drain the Alps to the east. In many downstream Danube tributaries in Hungary,
297 Romania and Bulgaria, on the other hand, streamflow droughts are projected to become more severe
298 (in agreement with the results reported in Stagl and Hattermann, 2015). At low levels of global
299 warming (1.5 and 2 K) most of Germany is expected to experience less severe droughts. At high
300 levels of warming (3 K), however, western parts of Germany are projected to experience and
301 inverse trend while the rest of the region shows a large uncertainty in the projected changes. In
302 contrast to most of the Continental sub-area, projections of streamflow drought severity show an
303 increase with global warming over the main rivers in Denmark.

304 Finally, in most of the Boreal region, streamflow drought deficits is expected to become
305 progressively less severe with warming. At 3 K warming streamflow droughts could be half as
306 severe compared to the baseline, with few notable exceptions in southern Sweden.

307 **3.1.2 Drought duration**

308 Figure 2 shows the fraction of each sub-region (presented in the lower-right panel of Figure 1)
309 for which a certain degree of change in drought duration (compared to the reference period) is
310 projected for the different warming levels. There is a clear upward climate change-induced trend in

311 the fraction of the Mediterranean sub-region that will be exposed to longer droughts with increasing
312 GWL. When keeping global warming limited to 1.5 K, droughts are projected to last more than 5-
313 days longer in about 40% of the Mediterranean, with a prolongation above 15 days in slightly more
314 than 5% of the area. At 3 K warming, however, streamflow droughts will last longer than in the
315 reference period in 80% of the area and nearly half of the sub-region could face an increase in
316 drought duration of at least 10 days.

317 An upward, but less pronounced, trend in drought duration with global warming is also
318 projected for most of the Atlantic sub-region. At 1.5 K GWL, the area with negative changes in
319 drought duration (about 30%) is comparable to the area with positive changes, with no clear signal
320 in about 40% of the domain. With higher levels of warming, the area with a shorter drought
321 duration compared to the reference shrinks, while the fraction of land that is expected to face longer
322 droughts steadily expands. Compared to 1981-2010, droughts are projected to last longer in about
323 75% of the sub-region at 3 K GWL, hence similar to what can be observed for the Mediterranean.
324 Yet, for only 10% of the area, drought duration is expected to increase by more than 10 days.

325 In the Continental sub-region, the area that shows a decrease in drought duration compared to
326 the reference period is around 65% at 1.5 K, which slightly reduces in extent with increasing
327 warming. Yet, over this area droughts are expected to progressively shorten with further warming.
328 At 3 K warming, with positive changes of at least 10 and 15 days over more than 30 and 10% of the
329 region, respectively. Drought duration is projected to increase over a small part (20% at 3 K) of the
330 domain compared to the reference period, mainly corresponding to Bulgaria.

331 Over the Boreal sub-region, droughts are projected to become shorter with global warming over
332 practically the whole domain. At 1.5 K warming, drought duration is expected to be at least 15 days
333 shorter than in 1981-2010 in 20% of the area, which grows to 50% of the area at 3 K warming. For
334 all sub-regions, the fraction of area with no-agreement in future drought duration changes tends to
335 reduce with increasing global warming, and this signal is very consistent among all the climate

336 projections. At 3 K warming, projections show that less than 15% of the domain under study have
337 no agreement in the direction of change in drought duration.

338 **3.1.3 Drought frequency**

339 Figure 3 shows the frequency density of drought return periods for the three GWLs
340 corresponding to an event with a return period (T) of 10 years under baseline climate. In these plots,
341 values greater than 10 can be interpreted as a reduction in drought frequency (an event with $T = 10$
342 years in the baseline will become rarer), whereas values lower than 10 represent an increase in
343 drought frequency (an event with $T = 10$ years in the baseline will become more common).

344 The frequency distributions of T values for the Mediterranean (upper-left panel) show a clear
345 shift towards more recurrent droughts. At 1.5 K warming the peak value is around 8 years, which
346 further reduces to 7 and 6 years at 2 and 3 K warming, respectively. At 3 K warming the lower tail
347 of the distribution falls below 4 years. In nearly 10% of the rivers, drought deficits that in baseline
348 climate happen once in 10 years are expected to occur at least 2.5 times more frequent with 3 K
349 warming. In the Atlantic sub-region the central value also reduces with warming, yet the overall
350 reduction is less pronounced than in the Mediterranean sub-area, with a median value around 7
351 years at 3 K warming. In the Continental region, droughts will in general become less frequent with
352 a central value between 12 and 13 years at all warming levels, even if the fraction of river cells with
353 an increase in frequency (around 28% at 3 K) is larger than that with an increase in drought duration
354 (less than 20% at 3 K, see Figure 2). In the Boreal sub-area the shift towards less frequent droughts
355 is much more pronounced, with projected return periods concentrated around 20, 30 and 40 years
356 for 1.5, 2 and 3 K warming, respectively.

357 Changes in the frequency density plots can be observed not only in the central tendency values,
358 but also in the spread, which increases with warming for all regions. Additionally, changes opposite
359 to the general trend can be observed in all regions. For example, over very few locations in the
360 Mediterranean sub-region, such as some Alpine mountain drainage basins in northern Italy, drought

361 conditions could become less severe and frequent (see also drought severity changes in Figure 1). In
362 the Atlantic region, the small secondary peak of T values > 20 years corresponds to areas where
363 droughts are projected to occur less frequently with global warming, such as Iceland and few
364 tributaries from the Rhône that originate in the Alps (similarly to what was observed on drought
365 severity in Figure 1). Even in the Boreal region a small fraction of the sub-domain shows an
366 increase in drought frequency, while drought duration is projected to reduce practically everywhere.
367 Over this region, the presence of small areas with increase in frequency causes a slight reduction in
368 the frequency median value at 3 K GWL (26 years, compared to 27 years at 2 K) even if the peak
369 shifts to the right with warming (i.e. less frequent droughts).

370 The results reported in Figure 3 for the 10-year return period can be seen as representative of
371 the behaviour at other return periods as well. To support this consideration, the data in Figure 4
372 report the sub-region median relative changes at the three GWLs for events with a baseline return
373 period of 3, 5, 10, 20 and 50 years. The plots clearly show how all the return periods have similar
374 dynamics, with the only notable exception represented by the more marked reduction in median
375 relative change of high return periods for the 3 K GWL in the Boreal sub-region (i.e., 20 and 50
376 years). It is also worth to point out how even if the dynamics are comparable among the different
377 return periods, the magnitude of the relative changes is higher for the longer return periods (i.e. the
378 rarer events).

379 ***3.2 Population and agricultural land exposed to drought***

380 Figure 5 shows the changes with respect to the baseline in population projected to be exposed to
381 streamflow drought at country scale (percentage relative changes are also reported as numbers next
382 to the bars). Total changes for the four macro-regions and the entire domain (TOTAL) are
383 summarised in Table 1. Aggregated over the whole domain, about 1.5 million fewer people are
384 expected to be annually exposed to drought at 1.5 K GWL compared to the baseline period, which
385 reverses to an increase of about 2.5 and 11 million people/year compared to baseline human

386 exposure at 2 and 3 K GWLs, respectively. This shift in the sign of the changes is caused by the fact
387 that at 1.5 K the increase in population exposed annually in the Mediterranean (2.4 million) and
388 Atlantic (less than 0.1 million) sub-regions is outweighed by the reduction in exposure in the Boreal
389 (-0.6 million) and, most importantly, Continental (-3.4 million) sub-regions. Projections in the
390 Mediterranean and Atlantic sub-regions show a progressive increase in population exposed (up to a
391 total of 15.8 million people/year for 3 K GWL over the two regions), while in the Boreal and
392 Continental combined human exposure to droughts is expected to remain roughly the same for all
393 three GWLs (i.e., -3.9, -5.4 and -4.7 million/year at 1.5, 2 and 3 K, respectively).

394 Spain is projected to have the largest absolute increase in population exposed to drought with
395 global warming, with an almost doubling (+3.8 million/year) of the number of people exposed to
396 drought each year at 3 K GWL. In relative terms, the relative increase in population exposure at 3K
397 is also high in Portugal (+81%), United Kingdom (+58%) and France (+52%). The largest absolute
398 decrease in population exposed is expected for Germany at 1.5 and 2 K GWL (-1.8 and -1.7 million
399 people/year) and Poland at 3 K GWL. The transition of several areas in Germany from a decrease in
400 drought to uncertain conditions (see as an example western Germany in Figure 1) explains the
401 lower number of exposed people at 3 K (-0.9 million people/year) compared to Poland (-1.2 million
402 people/year). The strongest reduction in population exposure in relative terms is expected for
403 Norway, Iceland and Lithuania (up to 65, 87 and 85%, respectively).

404 Exposure of agricultural land (Figure 6 and Table 2) shows similar trends as for population.
405 Aggregated over Europe, the change in exposure is projected to be balanced in the exposed
406 agricultural land at 1.5 K GWL (net increase of 0.1 million ha/year), whereas at higher warming
407 levels exposure of agricultural land increases to 1.2 and 4.5 million ha/year at 2 and 3 K,
408 respectively. This increasing trend in the Europe-average changes can be explained by the expected
409 steady increase in agricultural land exposed to drought in the Mediterranean and Atlantic sub-
410 regions (up to 6 million ha/year combined at 3 K), which is not counterbalanced at the highest
411 warming by the agricultural land being less exposed to drought in the Boreal and the Continental

412 sub-regions (-1.3 million ha/year at 1.5 K and -1.5 million ha/year at 3 K). In absolute numbers,
413 Spain shows the largest projected increase in the agricultural land exposed at all GWLs, with an
414 additional 0.9 million ha/year at 1.5 K to 2.6 million ha/year at 3 K (corresponding to a relative
415 increase of about 35 and 97%, respectively). Relative changes are expected to be quite notable for
416 other Mediterranean countries as well, such as Portugal and Greece, reaching almost 120 and 77%
417 at 3 K, respectively.

418 **4. Discussion**

419 The projections of severity, duration and frequency underline some common features in future
420 streamflow drought in Europe. The uncertainty in the projections is more marked at the 1.5 and 2 K
421 GWLs, whereas change patterns are more statistically robust at higher warming, as also observed by
422 Marx et al. (2018) for minimum flows. Overall, the magnitude of the projected changes increases
423 with warming for all the drought traits, with only limited areas interested by an inversion in the
424 trend. The main pattern is a strengthening of the dichotomy between south-western and north-
425 eastern Europe, with the already drought-prone south-west becoming even more prone to droughts
426 while the north-east will experience a further wetting. This result suggests a continuation of a trend
427 that is already ongoing according to Stagge et al. (2017), and it is also in line with other studies that
428 projected streamflow droughts focusing on specific time periods instead of GWLs (Lehner et al.,
429 2006; Feyen and Dankers, 2009; Stahl et al., 2012; Forzieri et al., 2014) or on agricultural (e.g.,
430 Samaniego et al., 2018) and meteorological (e.g., Gudmundsson and Seneviratne, 2016; Spinoni et
431 al., 2018) droughts. Hence, there is growing consensus in the community on the main patterns of
432 climate-induced changes on drought conditions in Europe.

433 Overall, the Mediterranean sub-region shows the strongest increase in drought traits, with
434 droughts projected to become more severe, last longer and happen more frequently already at 1.5 K
435 GWL. The combined effects of increasing temperature and decreasing summer precipitation
436 (Dubrovský et al., 2014; Vautard et al., 2014) are expected to result in a further exacerbation of

437 water deficits in an area already prone to limited water resources. This is particularly true during
438 summer, because of high water abstraction for irrigation (about 60% of the current water demand,
439 Vandecasteele et al., 2014). Studies that present future scenarios in agricultural water demand (i.e.
440 Chaturvedi et al., 2015; Schmitz et al., 2013) suggest that improvements in irrigation efficiency
441 could mitigate these impacts. Overall, the increasing pressure of drought on this region agrees with
442 global studies that identify the Mediterranean as a hot spot for climate change, even if the targets set
443 by the Paris agreement will be met (Gu et al., 2020), and also with the study of Guerreiro et al.
444 (2017) on the potential occurrence of multi-year droughts in major Iberian water resource regions.

445 In contrast, the Boreal sub-region is projected to experience a general reduction in all drought
446 traits, as the increase in precipitation will likely outweigh the increase in evaporative demand due to
447 elevated temperatures (Jacob et al., 2018). Over this region, similarly to the Alps (Donnelly et al.,
448 2017), increasing winter precipitation and higher temperatures are expected to result in higher
449 winter flows, when river flows are typically at their lowest (Gobiet et al., 2014). This result is
450 obtained in spite of the projected general increase in public water demand (the highest share of total
451 withdraws in northern Europe) and business-as-usual per capita water use (Vandecasteele et al.,
452 2014).

453 In the other two sub-regions the projections are less uniform, with more variation in the signal
454 and robustness of the projections with global warming. In the Atlantic sub-region the increase in
455 droughts at 3 K is expected to be less pronounced compared to the Mediterranean, but similarly
456 robust, while at lower warming levels there is large uncertainty in the projections. In some river
457 basins, such as the Seine in northern France, a decrease in droughts or uncertain trend is projected
458 for low levels of global warming, while at higher levels of warming drought conditions are
459 projected to worsen. This shift in the sign of the changes is likely related to the fact that at higher
460 levels of warming the atmospheric demand (evapotranspiration) rises faster than supply
461 (precipitation) due to the combination of a strong rise in temperature and a slight or uncertain
462 increase in annual precipitation and a decline in summer precipitation (Kotlarski et al., 2014). In the

463 Atlantic sub-region, areas with projected strong increase in population (e.g. southern UK,
464 EUROSTAT, 2019), are the ones with a clear increase in droughts for all warming levels. Given the
465 role of population in domestic water demand, changes over these regions seems to further
466 exacerbate the climate effects.

467 In the Continental sub-region the projected overall decrease in droughts is rather
468 inhomogeneous in strength. In upstream Danube tributaries draining the Alps there is a strong trend
469 towards less severe droughts as winter flows increase due to changes in snow accumulation and
470 melt caused by increased winter precipitation and higher temperatures (Forzieri et al., 2014; Marx et
471 al., 2018). In downstream reaches of the Danube, more severe droughts are projected due to a
472 reduction in summer flows caused by an increased evaporative demand and less precipitation, as
473 well as the reduced snowmelt contribution from the Alps (Jenicek et al., 2018). Also, in Germany,
474 the trend towards less severe droughts is reversed at higher warming as the increasing natural and
475 human demand in drier summers outbalance higher annual supply. The revert to increase in
476 droughts at 3 K GWL is the case especially in western parts of Germany such as downstream
477 reaches of the Rhine (Bosshard and Kotlarski, 2014).

478 The heterogeneity in the strength of the outcomes obtained over the Continental sub-region
479 further stress how the complex interplay between supply (precipitation), atmospheric demand
480 (evapotranspiration) and human water use can result in different projected trends. Dosio and Fischer
481 (2018) showed that precipitation will increase over most continental and northern parts of Europe
482 (by +10-25% at 3 K), but to a lesser extent in summer (changes with 3 K between -5% at middle
483 latitudes of Continental Europe to +10-15% at higher latitudes in the Boreal region), when natural
484 and human demand are highest. As a result, short duration droughts could happen more frequently
485 in some Eastern Europe catchments during summer even when supply does not change drastically
486 due to the growth in natural demand (because of rising temperatures) and the contextual steady
487 increase in human water demand for several socio-economic scenario (Ercin and Hoekstra, 2016).
488 In the case of longer drought events, the imbalances between supply and demand over summer may

489 be mitigated by the increase in subsurface storages at the start of the summer season due to elevated
490 precipitation amounts during the previous seasons, but also potentially exacerbated in case of multi-
491 annual summer droughts. In this context, human induced factors may influence drought propagation
492 even further in high-regulated European basins (Van Loon et al., 2016).

493 **5. Summary and Conclusions**

494 This study analysed how the main characteristics of hydrological droughts are expected to
495 change over Europe due to global warming. Projections in drought severity, duration and frequency
496 based on river water deficits highlight some common features and spatial patterns in future drought
497 conditions across Europe. The Mediterranean sub-region, which already suffers most from water
498 scarcity, is projected to experience the strongest effects of climate change on drought conditions.
499 With increasing global warming, streamflow deficits in this region are expected to happen more
500 frequently, become more severe and last longer. In contrast, the Boreal sub-area is projected to face
501 a consistent decrease in drought severity, duration and frequency.

502 In the Atlantic and Continental sub-regions the projections are less uniform, although over most
503 of the Atlantic drought conditions are projected to worsen, while they generally will become less
504 intense over Continental Europe. Despite the use of a large ensemble of climate models, there is still
505 a substantial uncertainty in the projections in these regions, even if changes at 3 K are mostly
506 statistically robust. The uncertainty is bigger for the 1.5 and 2 K GWLs, which suggests that there is
507 still large disagreement among the models in possible changes in drought conditions in these areas
508 when warming could be stabilised at the targets set in the Paris climate agreement. Since the climate
509 signal is less marked over these two sub-regions, projected water demand may play a more relevant
510 role in the direction of the future changes here. While in this study we considered water use
511 projections consistent with EU demographic, economic and energy projections, global and regional
512 water use studies show the large variability in future water use depending on the socioeconomic
513 scenario and water use model (Graham et al., 2018; Wada et al., 2016). Hence, apart from the

514 effects of warming on the hydrological cycle and natural water availability, socioeconomic
515 dynamics and consequent demand for water could also locally affect drought conditions.

516 Overall, the general patterns observed in this study are in line with the patterns observed in
517 studies that focused on specific temporal horizons rather than warming levels (Forzieri et al., 2014;
518 Spinoni et al., 2018; Stahl et al., 2012). Our study shows that with higher warming the changes in
519 drought traits are expected to be more marked, even if the spatial patterns of the areas with
520 increasing/decreasing drought conditions are rather similar for the three GWLs analysed here. The
521 outcomes obtained for different traits of streamflow droughts (i.e., severity, duration and frequency)
522 are in agreement with the results of Marx et al. (2018) based on the simple daily streamflow
523 percentile, suggesting again a strong coherence in streamflow climate projections.

524 The exposure analysis with population density and agricultural land highlights how at lower
525 warming levels positive and negative changes in exposure are expected to be balanced across
526 Europe. However, at higher GWLs the increase in population and agricultural land exposed in the
527 southern and western parts of Europe is projected to outweigh the effects of less severe droughts in
528 the less populated north and most of continental and eastern Europe. At 3 K warming this unbalance
529 between south-west and north-east could result in an additional 11 million people and 4.5 million ha
530 exposed each year to drought conditions that currently are expected to happen once every 10 years
531 or less frequently. The projected changes in exposure to drought will pose considerable challenges
532 for agriculture and water provision in densely populated and economically pivotal areas, especially
533 in southern Europe, making the findings of this study relevant to provide information that can be
534 used as a basis to evaluate the implications at European scale of climate mitigation policies.

535

536 **Data availability.** All data are freely available to the public via the EDO web portal
537 (<https://edo.jrc.ec.europa.eu/>) upon request. The main outputs of the study will be made available
538 through the JRC-DRMKC Risk Data Hub (<https://drmkc.jrc.ec.europa.eu/risk-data-hub>).

539 **References**

- 540 Arnal, L., Asp, S.-S., Baugh, C., de Roo, A., Disperati, J., Dottori, F., Garcia, R., GarciaPadilla, M.,
541 Gelati, E., Gomes, G., Kalas, M., Krzeminski, B., Latini, M., Lorini, V., Mazzetti, C.,
542 Mikulickova, M., Muraro, D., Prudhomme, C., Rauthe-Schöch, A., Rehfeldt, K., Salamon,
543 P., Schweim, C., Skoien, J. O., Smith, P., Sprokkereef, E., Thiemig, V., Wetterhall, F.,
544 Ziese, M., 2019. EFAS upgrade for the extended model domain – technical documentation.
545 JRC Technical Reports, EUR 29323 EN, Publications Office of the European Union,
546 Luxembourg, 58 pp. doi:10.2760/806324.
- 547 Barker, L.J., Hannaford, J., Chiverton, A., Svensson, C., 2016. From meteorological to hydrological
548 drought using standardised indicators. *Hydrol. Earth Syst. Sci.* 20, 2483-2505.
549 doi:10.5194/hess-20-2483-2016.
- 550 Batista e Silva, F., Gallego, J., Lavallo, C., 2013. A high-resolution population grid map for Europe.
551 *J. Maps* 9(1), 16-28. doi: 10.1080/17445647.2013.764830.
- 552 Bisselink, B., Bernhard, J., Gelati, E., Adamovic, M., Guenther, S., Mentaschi, L., De Roo, A.,
553 2018. Impact of a changing climate, land use, and water usage on Europe's water resources.
554 JRC Technical Reports, EUR 29130 EN, Publications Office of the European Union,
555 Luxembourg, 86 pp. doi:10.2760/847068.
- 556 Bosshard, T., Kotlarski, S., 2014. Hydrological climate-impact projections for the Rhine river:
557 GCM–RCM uncertainty and separate temperature and precipitation effects. *Hydrometeor.*
558 15, 697-713. doi:10.1175/JHM-D-12-098.1.
- 559 Brunner, M.I., Liechti, K., Zappa, M., 2019. Extremeness of recent drought events in Switzerland:
560 Dependence on variable and return period choice. *Nat. Hazards Earth Syst. Sci.* 19(10),
561 2311-2323. doi:10.5194/nhess-19-2311-2019.

562 Burek, P., van der Knijff, J.M., De Roo, A., 2013. LISFLOOD: Distributed Water Balance and
563 Flood Simulation Model. JRC Technical Reports, EUR 26162 EN, Publications Office of
564 the European Union, Luxembourg, 142 pp. doi:10.2788/24719.

565 Cammalleri, C., Vogt, J., Salamon, P., 2017. Development of an operational low-flow index for
566 hydrological drought monitoring over Europe. *Hydrol. Sci. J.* 62(3), 346-358.
567 doi:10.1080/02626667.2016.1240869.

568 Cammalleri, C., Barbosa, P., Vogt, J.V., 2020. Evaluating simulated daily discharge for operational
569 hydrological drought monitoring in the Global Drought Observatory (GDO), *Hydrol. Sci. J.*
570 65(8), 1316-1325. doi:10.1080/02626667.2020.1747623.

571 Capros, P., Van Regemorter, D., Paroussos, L., Karkatsoulis, P., 2013. GEM-E3 model
572 documentation. JRC Technical Reports, EUR 26034 EN, Publications Office of the
573 European Union, Luxembourg, 158 pp. doi:10.2788/47872.

574 Cervi, F., Petronici, F., Castellarin, A., Marcaccio, M., Bertolini, A., Borgatti, L., 2018. Climate-
575 change potential effects on the hydrological regime of freshwater springs in the Italian
576 northern Apennines. *Sci. Total Environ.* 622-623, 337-348.
577 doi:10.1016/j.scitotenv.2017.11.231.

578 Chaturvedi, V., Hejazi, M., Edmonds, J., Clarke, L., Kyle, P., Davies, E., Wise, M., 2015. Climate
579 mitigation policy implications for global irrigation water demand. *Mitig. Adapt. Strat. Global*
580 *Change* 20(3), 389-407. doi:10.1007/s11027-013-9497-4.

581 Chow, V.T., Maidment, D., Mays, L.W., 1988. *Applied Hydrology*. New York, McGraw-Hill.

582 Crausbay, S.D., Ramirez, A.R., 2017. Defining ecological drought for the twenty-first century. *Bull.*
583 *Am. Meteorol. Soc.* 2543-2550. doi:10.1175/BAMS-D-16-0292.1.

584 De Roo, A., Wesseling, C., Van Deursen, W., 2000. Physically based river basin modelling within
585 a GIS: the LISFLOOD model. *Hydrol. Process.* 14, 1981-1992. doi:10.1002/1099-1085.

586 Donnelly, C., Greuell, W., Andersson, J., Gerten, D., Pisacane, G., Roudier, P., Ludwig, F., 2017.
587 Impacts of climate change on European hydrology at 1.5, 2 and 3 degrees mean global
588 warming above preindustrial level. *Climatic Change* 143, 13-26. doi:10.1007/s10584-017-
589 1971-7.

590 Dosio, A., 2020. Mean and extreme climate in Europe under 1.5, 2, and 3°C global warming. EUR
591 30194 EN, Publications Office of the European Union, Luxembourg, 2020, ISBN 978-92-
592 76-18430-0, doi:10.2760/826427, JRC120574.

593 Dosio, A., Fischer, E.M., 2018. Will half a degree make a difference? Robust projections of indices
594 of mean and extreme climate in Europe under 1.5°C, 2°C, and 3°C global warming. *Geoph.*
595 *Res. Letters* 45(2), 935-944. doi:10.1002/2017GL076222.

596 Dosio, A., Paruolo, P., Rojas, R., 2012. Bias correction of the ENSEMBLES high resolution
597 climate change projections for use by impact models: Analysis of the climate change signal.
598 *J. Geoph. Res. Atm.* 117(17). doi:10.1029/2012JD017968.

599 Dubrovský, M., Hayes, M., Duce, P., Trnka, M., Svoboda, M., Zara, P., 2014. Multi-GCM
600 projections of future drought and climate variability indicators for the Mediterranean region.
601 *Reg. Environ. Change* 14, 1907-1919. doi:10.1007/s10113-013-0562-z.

602 EC, 2015. The 2015 Ageing Report - Economic and budgetary projections for the 28 EU Member
603 States (2013-2060). European Commission. doi:10.2765/877631.

604 EEA, 2016. Corine Land Cover (CLC), Version 18.5.1. Release Date: 19-09-2016. European
605 Environment Agency. <https://land.copernicus.eu/pan-european/corine-land-cover>.

606 Ercin, A. E., Hoekstra, A. Y., 2016. European Water Footprint Scenarios for 2050. *Water* 8(6), 226.
607 doi:10.3390/w8060226.

608 EUROSTAT, 2019. [https://ec.europa.eu/eurostat/statistics-
609 explained/index.php?title=Archive:Statistics_on_regional_population_projections#Projected
610 changes_in_regional_populations](https://ec.europa.eu/eurostat/statistics-explained/index.php?title=Archive:Statistics_on_regional_population_projections#Projected_changes_in_regional_populations), last access: 11 September 2020.

611 Feng, S., 2017. Why do different drought indices show distinct future drought risk outcomes in the
612 U.S. Great Plains? *J. Climate* 30, 265-278. doi: 10.1175/JCLI-D-15-0590.1.

613 Feyen, L., Dankers, R., 2009. Impact of global warming on streamflow drought in Europe. *J.*
614 *Geophys. Res.* 114, D17116. doi:10.1029/2008JD011438.

615 Forzieri, G., Feyen, L., Rojas, R., Flörke, M., Wimmer, F., Bianchi, A., 2014. Ensemble projections
616 of future streamflow droughts in Europe. *Hydrol. Earth Syst. Sci.* 18(1), 85-108.
617 doi:10.5194/hess-18-85-2014.

618 Gobiet, A., Kotlarski, S., Beniston, M., Heinrich, G., Rajczak, J., Stoffel, M., 2014. 21st century
619 climate change in the European Alps - A review. *Sci. Tot. Environ.* 493, 1138-1151.
620 doi:10.1016/j.scitotenv.2013.07.050.

621 Gu, L., Chen, J., Yin, J., Sullivan, S.C., Wang, H.-M., Guo, S., Zhang, L., Kim, J.-S., 2020.
622 Projected increases in magnitude and socioeconomic exposure of global droughts in 1.5 and
623 2 °C warmer climates. *Hydrol. Earth Syst. Sci.* 24, 451-472. doi:10.5194/hess-24-451-2020.

624 Gudmundsson, L., Seneviratne, S.I., 2016. Anthropogenic climate change affects meteorological
625 drought risk in Europe. *Environ. Res. Lett.* 11, 044005. doi:10.1088/1748-
626 9326/11/4/044005.

627 Guerreiro, S.B., Birkinshaw, S., Kilsby, C., Fowler, H.J., Lewis, E., 2017. Dry getting drier – The
628 future of transnational river basins in Iberia. *J. Hydrol. Reg. Studies* 12, 238-252.
629 doi:10.1016/j.ejrh.2017.05.009.

630 Gupta, H. V., Kling, H., Yilmaz, K. K., Martinez, G. F., 2009. Decomposition of the mean squared
631 error and NSE performance criteria: Implications for improving hydrological modelling. *J.*
632 *Hydrol.* 377(1-2), 80-91. doi: 10.1016/j.jhydrol.2009.08.003.

633 Haylock, M.R., Hofstra, N., Klein Tank, A.M.G., Klok, E.J., Jones, P.D., New, M., 2008. A
634 European daily high-resolution gridded data set of surface temperature and precipitation for
635 1950–2006. *J. Geoph. Res.* 113, D20119. doi:10.1029/ 2008JD010201.

636 Heinrich, G., Gobiet, A., 2012. The future of dry and wet spells in Europe: a comprehensive study
637 based on the ENSEMBLES regional climate models. *Int. J. Climatol.* 32(13), 1951-1970.
638 doi:10.1002/joc.2421.

639 Hellwig, J., Stahl, K., 2018. An assessment of trends and potential future changes in groundwater-
640 baseflow drought based on catchment response times. *Hydrol. Earth Syst. Sci.* 22(12), 6209-
641 6224. doi:10.5194/hess-22-6209-2018.

642 Hirpa, F.A., Salamon, P., Beck, H.E., Lorini, V., Alfieri, L., Zsoter, E., Dadson, S.J., 2018.
643 Calibration of the Global Flood Awareness System (GloFAS) using daily streamflow data. *J.*
644 *Hydrol.* 566, 595-606. doi: 10.1016/j.jhydrol.2018.09.052.

645 Jacob, D., Petersen, J., Eggert, B., Alias, A., Christensen, O.B., Bouwer, L.M., Braun, A., Colette,
646 A., Déqué, M., Georgievski, G., Georgopoulou, E., Gobiet, A., Menut, L., Nikukin, G.,
647 Haensler, A., Hempelmann, N., Jones, C., Keuler, K., Kovats, S., Kröner, N., Kotlarski, S.,
648 Kriegsmann, A., Martin, E., Van Meijgaard, E., Moseley, C., Pfeifer, S., Preuschmann, S.,
649 Radermacher, C., Radtke, K., Rechid, D., Rounsevell, M., Samuelsson, P., Somot, S.,
650 Soussana, J.-F., Teichmann, C., Valentini, R., Vautard, R., Weber, B., Yiou, P., 2014. EURO-
651 CORDEX: New high-resolution climate change projections for European impact research.
652 *Reg. Environ Change* 14(2), 563-578. doi:10.1007/s10113-013-0499-2.

653 Jacob, D., Kotova, L., Teichmann, C., Sobolowski, S.P., Vautard, R., Donnelly, C., Koutroulis,
654 A.G., Grillakis, M.G., Tsanis, I.K., Damm, A., Sakalli, A., Van Vliet, M.T.H., 2018. Climate
655 Impacts in Europe Under +1.5°C Global Warming. *Earth's Future* 6, 264-285.
656 doi:10.1002/2017EF000710.

657 Jacobs-Crisioni, C., Diogo, V., Perpiña Castillo, C., Baranzelli, C., Batista e Silva, F., Rosina, K.,
658 Kavalov, B., Lavallo, C., 2017. The LUISA Territorial Reference Scenario 2017: A technical
659 description. JRC Technical Reports, EUR 28800 EN, Publications Office of the European
660 Union, Luxembourg, 46 pp. doi:10.2760/902121.

661 Jakubowski, W., Radczuk, L., 2004. Estimation of hydrological drought characteristics
662 NIZOWKA2003 – Software Manual. In: L.M. Tallaksen and H.A.J. van Lanen, eds.
663 Hydrological Drought – Processes and estimation methods for Streamflow and groundwater.
664 Amsterdam: Elsevier Sciences B.V. [CD-ROM].

665 Jenicek, M., Seibert, J., Staudinger, M., 2018. Modeling of future changes in seasonal snowpack
666 and impacts on summer low flows in Alpine catchments. *Water Resour. Res.* 54(1), 538-556.
667 doi:10.1002/2017WR021648.

668 Keramidas, K., Kitous, A., Després, J., Schmitz, A., 2017. POLES-JRC model documentation. EUR
669 28728 EN, Publications Office of the European Union, Luxembourg. ISBN 978-92-79-71801-
670 4. doi:10.2760/225347, JRC107387.

671 Kotlarski, S., Keuler, K., Christensen, O. B., Colette, A., Déqué, M., Gobiet, A., Wulfmeyer, V.,
672 2014. Regional climate modeling on European scales: A joint standard evaluation of the
673 EURO - CORDEX RCM ensemble. *Geosci. Model Develop.* 7(4), 1297-1333.
674 doi:10.5194/gmd-7-1297-2014.

675 Kovats, R., Valentini, R., Bouwer, L., Georgopoulou, E., Jacob, D., Martin, E., Rounsevell, M.,
676 Soussana, J.-F., 2014. Europe, In: *ClimateChange 2014: Impacts, Adaptation, and*
677 *Vulnerability. Part B: Regional Aspects. Contribution of Working Group II to the Fifth*
678 *Assessment Report of the Intergovernmental Panel on Climate Change*, Eds: Barros, V.R.,
679 C.B. Field, D.J. Dokken, M.D. Mastrandrea, K.J. Mach, T.E. Bilir, M. Chatterjee, K.L. Ebi,
680 Y.O. Estrada, R.C. Genova, B. Girma, E.S. Kissel, A.N. Levy, S. MacCracken, P.R.
681 Mastrandrea, L.L. White, pp. 1267–1326.

682 Lehner, B., Döll, P., Alcamo, J., Henrichs, T., Kaspar, F., 2006. Estimating the impact of global
683 change on flood and drought risks in Europe: a continental integrated analysis. *Clim.*
684 *Change* 75, 273-299. doi:10.1007/s10584-006-6338-4.

685 Lomax, K., 1987. Business failures: another example of the analysis of failure data. *J. Am. Stat.*
686 *Assoc.* 49, 847-852. doi:10.2307/2281544.

687 Marx, A., Kumar, R., Thober, S., Rakovec, O., Wanders, N., Zink, M., Wood, E.F., Pan, M.,
688 Sheffield, J., Samaniego, L., 2018. Climate change alters low flows in Europe under global
689 warming of 1.5, 2, and 3 °C. *Hydrol. Earth Syst. Sci.* 22, 1017-1032. doi:10.5194/hess-22-
690 1017-2018.

691 Mentaschi, L., Alfieri, L., Dottori, F., Cammalleri, C., Bisselink, B., De Roo, A., Feyen, L., 2020.
692 Independence of future changes of river runoff in Europe from the pathway to global
693 warming. *Climate*, 8, 22. doi:10.3390/cli8020022.

694 Metzger, M.J., Bunce, R.G.H., Jongman, R.H.G., Múcher, C.A., Watkins, J.W., 2005. A climatic
695 stratification of the environment of Europe. *Glob. Ecol. Biogeogr.* 14, 549–563.
696 doi:10.1111/j.1466-822X.2005.00190.x.

697 Meyer, V., Becker, N., Markantonis, V., Schwarze, R., van der Bergh, J.C.J.M., Bouwer, L.M.,
698 Bubeck, P., Ciavola, P., Genovese, E., Green, C., Hallagatte, S., Kreibich, H., Lequex, Q.,
699 Logar, I., Papyrakis, E., Pfuerscheller, C., Poussin, J., Przulski, V., Thielen, A.H.,
700 Viavattene, C., 2013. Assessing the costs of natural hazards – state of the art and knowledge
701 gaps. *Nat. Hazard Earth Syst. Sci.* 13(5), 1351-1373. doi:10.5194/nhess-13-1351-2013.

702 Moss, R.H. et al., 2010. The next generation of scenarios for climate change research and
703 assessment. *Nature* 463(7282), 747-756. doi:10.1038/nature08823.

704 Mubareka, S., Maes, J., Lavalle, C., De Roo, A., 2013. Estimation of water requirements by
705 livestock in Europe. *Ecosyst. Serv.* 4, 139-145. doi:10.1016/j.ecoser.2013.03.001.

706 Nerantzaki, S. D., Efstathiou, D., Giannakis, G.V., Kritsotakis, M., Grillakis, M.G., Koutroulis, A.
707 G., Tsanis, I.K., Nikolaidis, N.P., 2019. Climate change impact on the hydrological budget
708 of a large Mediterranean island. *Hydrol. Sci. J.* 64(10), 1190-1203.
709 doi:10.1080/02626667.2019.1630741.

710 Roudier, P., Andersson, J.C.M., Donnelly, C., Feyen, L., Greuell, W., Ludwig, F., 2016. Projections
711 of future floods and hydrological droughts in Europe under a +2°C global warming.
712 *Climatic Change* 135(2), 341-355. doi:10.1007/s10584-015-1570-4.

713 Rudd, A.C., Kay, A.L., Bell, V.A., 2019. National-scale analysis of future river flow and soil
714 moisture droughts: Potential changes in drought characteristics. *Clim. Change* 156(3), 323-
715 340. doi:10.1007/s10584-019-02528-0.

716 Samaniego, L., Thober, S., Kumar, R., Wanders, N., Rakovec, O., Pan, M., Zink, M., Sheffield, J.,
717 Wood, E.F., Marx, A., 2018. Anthropogenic warming exacerbates European soil moisture
718 droughts. *Nat. Clim. Change* 8, 421-426. doi:10.1038/s41558-018-0138-5.

719 Schmitz, C., Lotze-Campen, H., Gerten, D., Dietrich, J.P., Bodirsky, B., Biewald, A., Popp, A.,
720 2013. Blue water scarcity and the economic impacts of future agricultural trade and demand.
721 *Water Resour. Res.* 49(6), 3601-3617. doi:10.1002/wrcr.20188.

722 Serinaldi, F., 2015. Dismissing return periods! *Stoch. Environ. Res. Risk Assess.* 29, 1179-1189.
723 doi:10.1007/s00477-014-0916-1.

724 Spinoni, J., Vogt, J.V., Naumann, G., Barbosa, P., Dosio, A., 2018. Will drought events become
725 more frequent and severe in Europe? *Int. J. Climatol.* 38(4), 1718-1736.
726 doi:10.1002/joc.5291.

727 Stagge, J.H., Kingston, D.G., Tallaksen, L.M., Hannah, D.M., 2017. Observed drought indices
728 show increasing divergence across Europe. *Sci. Rep.* 7, 14045. doi:10.1038/s41598-017-
729 14283-2.

730 Stagl J., Mayr E., Koch H., Hattermann F.F., Huang S., 2014. Effects of climate change on the
731 hydrological cycle in Central and Eastern Europe. In: Rannow S. and Neubert M. (eds.)
732 *Managing Protected Areas in Central and Eastern Europe Under Climate Change. Advances*
733 *in Global Change Research* 58. Springer, Dordrecht.

734 Stagl J., Hattermann F.F., 2014. Impacts of climate change on the hydrological regime of the
735 Danube river and its tributaries using an ensemble of climate scenarios. *Water* 7(11), 6139-
736 6172, doi:10.3390/w7116139.

737 Stahl, K., Tallaksen, L. M., Hannaford, J., and van Lanen, H. A. J., 2012. Filling the white space on
738 maps of European runoff trends: estimates from a multi-model ensemble. *Hydrol. Earth*
739 *Syst. Sci.* 16, 2035-2047. doi:10.5194/hess-16-2035-2012.

740 Tallaksen, L.M., Van Lanen, H.A.J., 2004. Drought as natural hazard: Introduction. In: L.M.
741 Tallaksen and H.A.J. Van Lanen, (eds.) *Hydrological Drought - Processes and estimation*
742 *methods for streamflow and groundwater*. Amsterdam: Elsevier Sciences B.V., 3-17.

743 Tebaldi C., Arblaster J.M., Knutti, R., 2011. Mapping model agreement on future climate
744 projections. *Geophys Res. Lett.* 38, L23701. doi:10.1029/2011G L0498 63.

745 Teuling, A.J., Van Loon, A.F., Seneviratne, S.I., Lehner, I., Aubinet, M., Heinesch, B., Bernhofer,
746 C., Grünwald, T., Prasse, H., Spank, U., 2013. Evapotranspiration amplifies European
747 summer drought. *Geophys. Res. Letters* 40(10), 2071-2075. doi:10.1002/grl.50495.

748 UNFCCC, 2015. The Paris Agreement. United Nations Framework Convention on Climate Change.
749 Available at: [https://unfccc.int/process-and-meetings/the-paris-agreement/the-paris-](https://unfccc.int/process-and-meetings/the-paris-agreement/the-paris-agreement)
750 [agreement](https://unfccc.int/process-and-meetings/the-paris-agreement/the-paris-agreement).

751 Vandecasteele, I., Bianchi, A., Batista e Silva, F., Lavallo, C., Batelaan, O., 2014. Mapping current
752 and future European public water withdrawals and consumption. *Hydrol. Earth Syst. Sci.* 18,
753 407-416. doi:10.5194/hess-18-407-2014.

754 Van Loon, A.F., Van Lanen, H.A.J., 2012. A process-based typology of hydrological drought.
755 *Hydrol. Earth Syst. Sci.* 16, 1915-1946. doi:10.5194/hess-16-1915-2012.

756 Van Loon, A.F., Van Lanen, H.A.J., 2013. Making the distinction between water scarcity and
757 drought using an observation - modeling framework. *Water Resour. Res.* 49, 1483-1502,
758 doi:10.1002/wrcr.20147.

759 Van Loon, A., Gleeson, T., Clark, J., Van Dijk, A.I.J.M., Stahl, K., Hannaford, J., Di Baldassarre,
760 G., Teuling, A.J., Tallaksen, L.M., Uijlenhoet, R., Hannah, D.M., Sheffield, J., Svoboda, M.,
761 Verdeiren, B., Wagener, T., Rangecroft, S., Wanders, N., Van Lanen, H.A.J., 2016. Drought
762 in the Anthropocene. *Nat. Geosci.* 9, 89-91. doi:10.1038/ngeo2646.

763 Van Tiel, M., Teuling, A.J., Wanders, N., Vis, M.J.P., Stahl, K., Van Loon, A.F., 2018. The role of
764 glacier changes and threshold definition in the characterisation of future streamflow
765 droughts in glacierised catchments. *Hydrol. Earth Syst. Sci.* 22(1), 463-485.
766 doi:10.5194/hess-22-463-2018.

767 Vautard, R., Gobiet, A., Sobolowski, S., Kjellström, E., Stegehuis, A., Watkiss, P., Mendlik, T.,
768 Landgren, O., Nikulin, G., Teichmann, C., Jacob, D., 2014. The European climate under a
769 2 °C global warming. *Environ. Res. Lett.* 9, 034006. doi:10.1088/1748-9326/9/3/034006.

770 Wada, Y., Flörke, M., Hanasaki, N., Eisner, S., Fischer, G., Tramberend, S., Satoh, Y., van Vliet,
771 M. T. H., Yillia, P., Ringler, C., Burek, P., Wiberg, D., 2016. Modeling global water use for
772 the 21st century: the Water Futures and Solutions (WFaS) initiative and its approaches.
773 *Geosci. Model Dev.* 9, 175-222. doi: 10.5194/gmd-9-175-2016.

774 Wilhite, D.A., 2000. Drought as a natural hazard: concepts and definitions. In: Wilhite D.A., (eds.)
775 *Droughts: Global Assessment*. London: Routledge, 3-18.

776 Yevjevich, V., 1967. An objective approach to definitions and investigations of continental
777 hydrological droughts. Colorado State University, Fort Collins, Hydrology Paper 23.

778 Zelenhasić, E., Salvai, A., 1987. A method of streamflow drought analysis. *Water Resour. Res.*,
779 23(1), 156-168. doi:10.1029/WR023i001p00156.

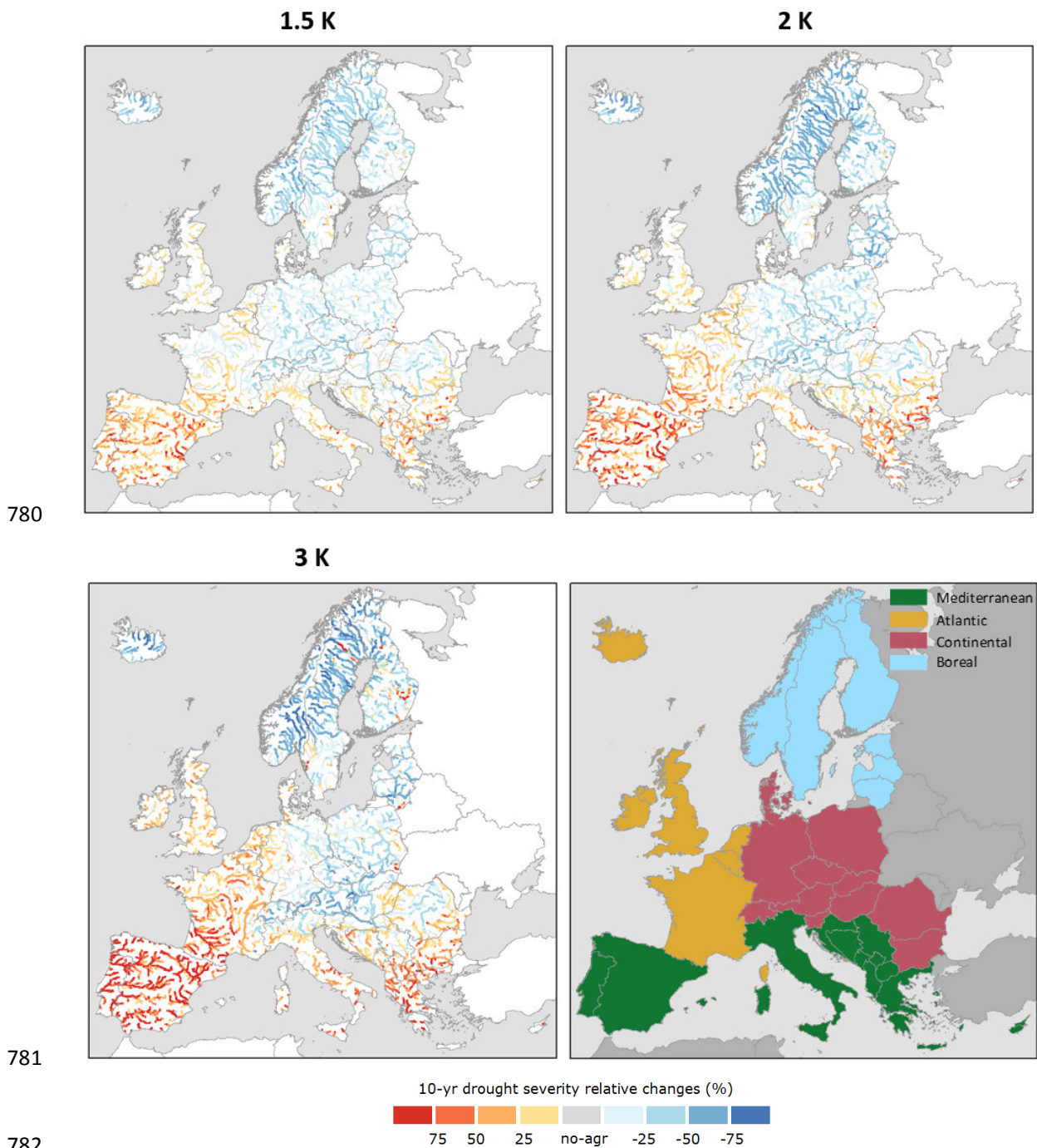
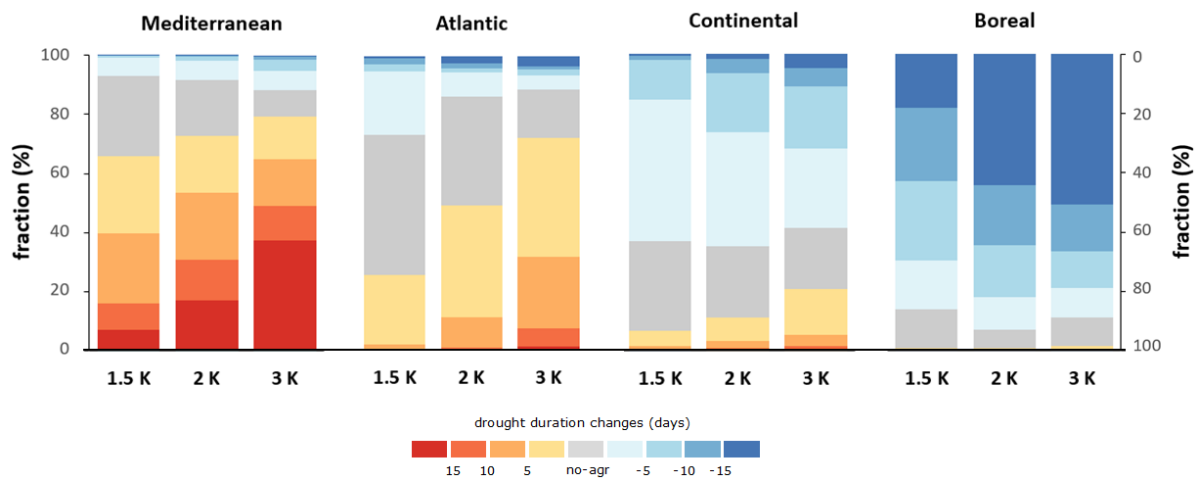
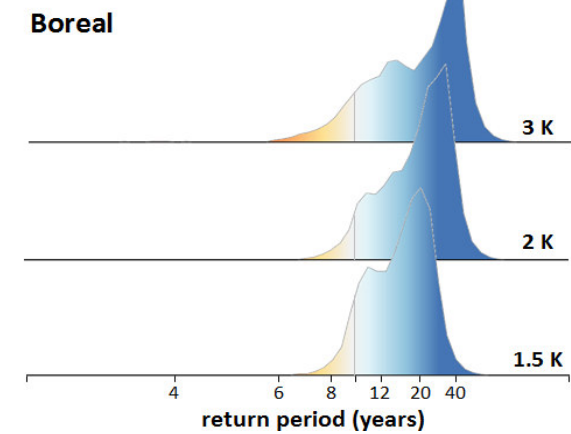
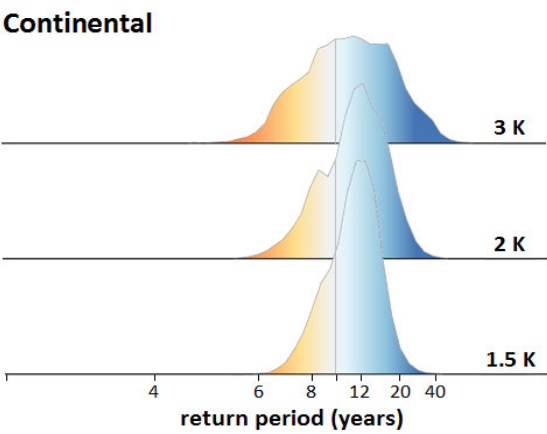
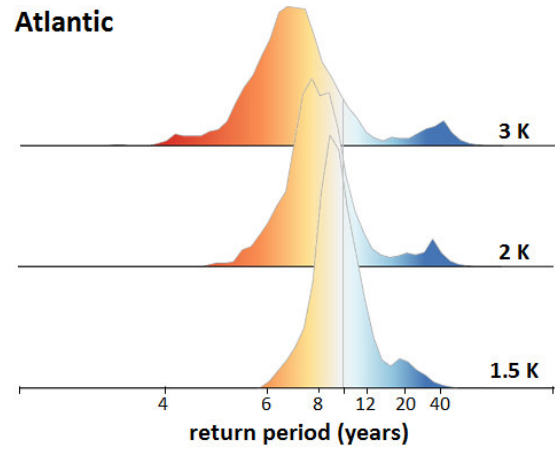
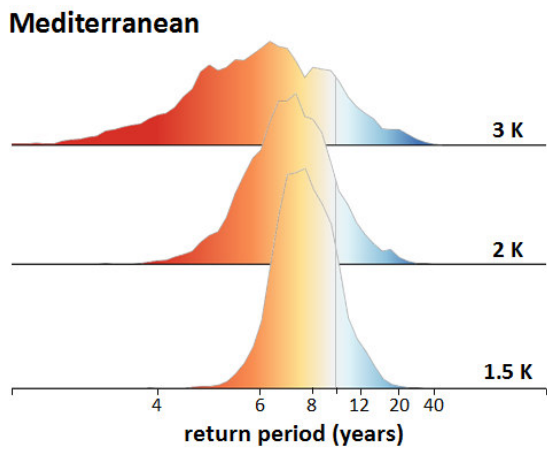


Fig. 1. Spatial distribution of the ensemble-median relative changes in drought severity of a 10-year drought (%) between reference period and the three GWLs (1.5 K in the upper-left panel, 2 K in the upper-right panel, 3 K in the lower-left panel). Positive values represent an increase in drought severity with warming. The no-agreement (no-agr) class identifies the cells where less than 2/3 of the climate ensemble members agree on the sign of the change. The lower-right panel represents the four sub-regions used for aggregation, which are in line with the IPCC AR5 European macro regions (Kovats et al., 2014).



790

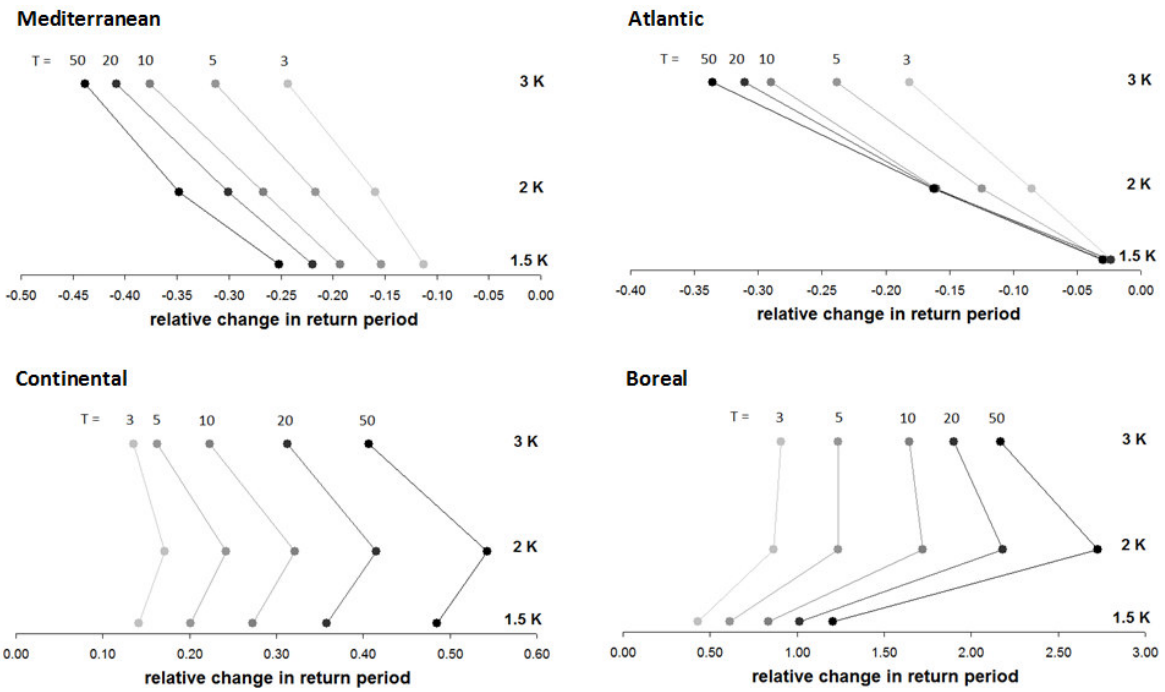
791 **Fig. 2.** Fraction of each sub-region within ranges of change in drought duration (days) for different
 792 GWLs. Note that two y-axes are added to the figure only to facilitate the interpretation of the
 793 positive (left axis) and negative (right axis) fraction values.



794

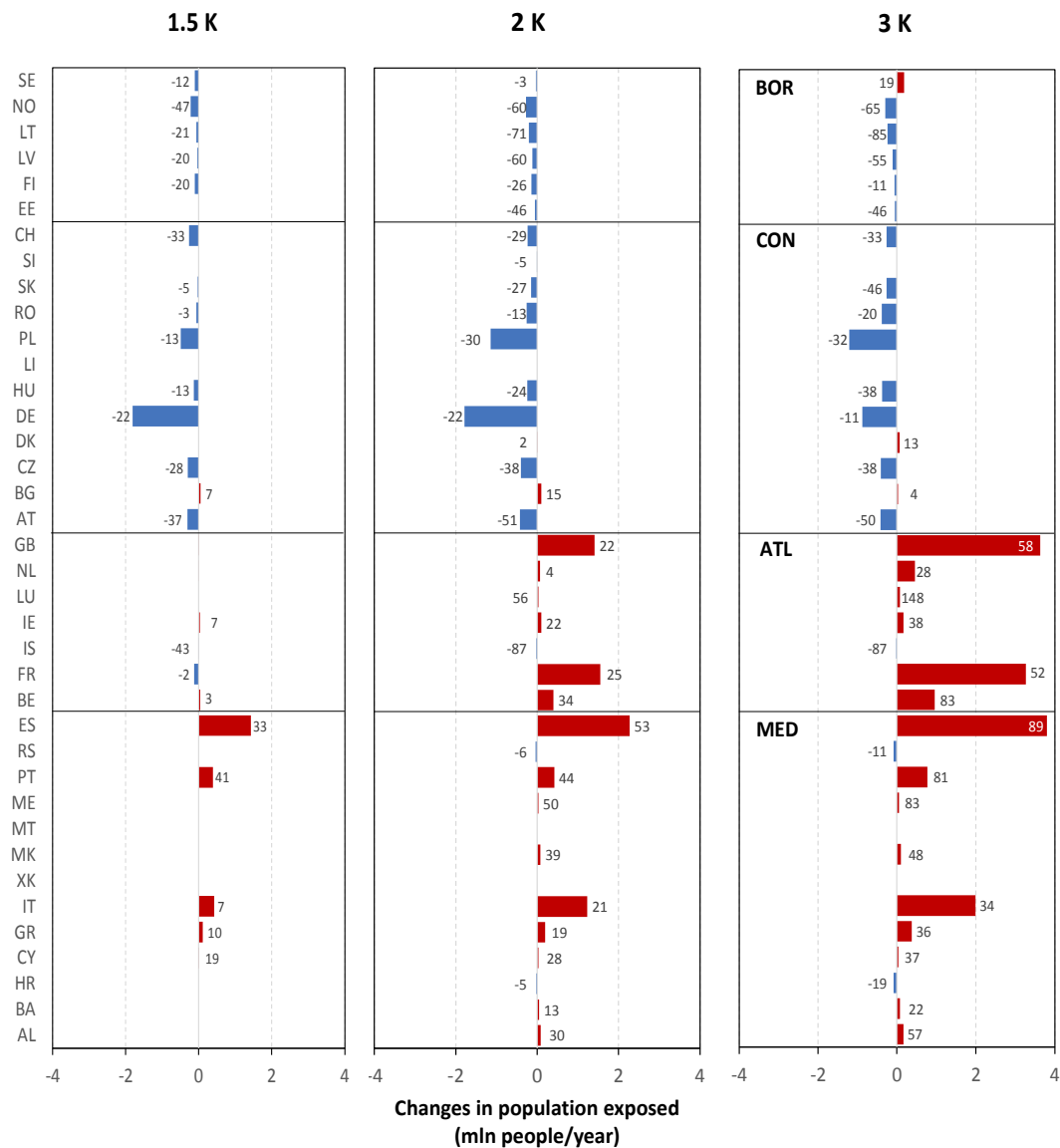
795

796 **Fig. 3.** Frequency distribution of the return period (years) for different GWLs corresponding to an
 797 event with a return period of 10 years in the reference baseline. Values lower (higher) than 10
 798 represent an increase (reduction) in drought frequency. The vertical grey lines demark the 10-year
 799 return period, and the tick marks are uniformly spaced in frequency.



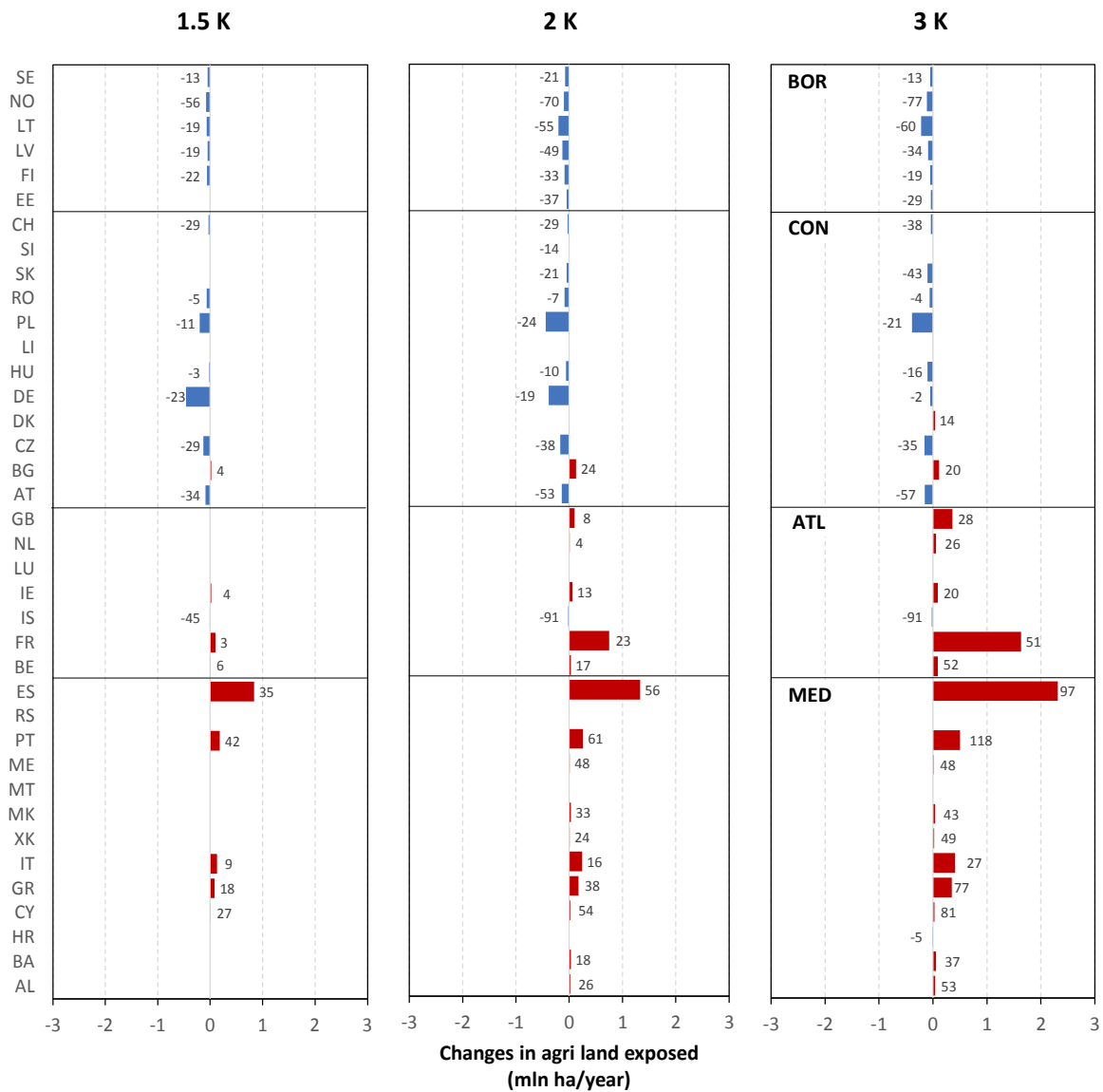
800

801 **Fig. 4.** Relative changes in sub-regional median return period (years) for different GWLs
 802 corresponding to events with a return period of 3, 5, 10, 20 and 50 years in the reference baseline.
 803 Negative (positive) values represent an increase (reduction) in drought frequency. Note that the x-
 804 axis scale is different for each plot.



805

806 **Fig. 5.** Changes in population exposed per country (million people/year). Positive values indicate an
 807 increase in the population exposed. The numbers near the bars represent the percentage changes
 808 relative to the baseline (only if greater than 1%).



809

810 **Fig. 6.** Changes in agricultural land exposed per country (million ha/year). Positive values indicate
 811 an increase in the area exposed. The numbers near the bars represent the percentage changes
 812 relative to the baseline (only if greater than 1%).

813 **Table 1.** Total population exposed per sub-regions (million people/year).

Name	baseline	1.5 K	2 K	3 K
MEDITERRANEAN	14.4	16.8	18.8	21.7
ATLANTIC	16.0	16.1	19.5	24.5
CONTINENTAL	19.6	16.2	15.0	15.5
BOREAL	2.5	2.0	1.7	1.9
TOTAL	52.5	51.1	55.0	63.6

814

815 **Table 2.** Total agricultural land exposed per sub-regions (million ha/year).

Name	baseline	1.5 K	2 K	3 K
MEDITERRANEAN	5.8	7.1	8.0	9.6
ATLANTIC	5.4	5.5	6.3	7.6
CONTINENTAL	7.7	6.8	6.5	6.8
BOREAL	1.6	1.3	0.9	1.0
TOTAL	20.5	20.6	21.7	25.0

816